ELSEVIER

Biochimica et Biophysica Acta 1513 (2001) 63–74

BIOCHIMICA ET BIOPHYSICA ACTA
BBA

www.bba-direct.com

Molecular dynamics simulations of the insertion of two ideally amphipathic lytic peptides LK_{15} and LK_9 in a 1,2-dimyristoylphosphatidylcholine monolayer

Céline Escrive, Michel Laguerre *

Institut Européen de Chimie et de Biologie (IECB – Ecole Polytechnique), 16 Avenue Pey-Berland, 33607 Pessac Cedex, France

Received 11 October 2000; received in revised form 24 April 2001; accepted 24 April 2001

Abstract

We present here the results of 1-ns molecular dynamics (MD) simulations of two ideally amphipathic lytic peptides, namely LK_{15} and LK_9, in a 1,2-dimyristoylphosphatidylcholine monolayer with two different cross-sectional areas per lipid of 80 $Å^2$ (loose film) and 63 $Å^2$ (tight standard film). These peptides are lytic, ideally amphipathic with a minimalist composition L_iK_j and the following sequences: H_2N-KLLKLLLKLLLKLLK-CO-Ph for LK_{15} and H_2N-KLKLKLKLK-CO-Ph for LK_9. From experimental data, LK_{15} exhibits an α-helical secondary structure, whereas LK_9 was found to form antiparallel β-sheets at the interface of a DMPC monolayer. Whatever the specific lipid surface is, the two peptides exhibit very different behavior: the α-helix inserts deeply into the monolayer whereas the β-sheeted peptide stays at the surface within the upper polar part of the monolayer. In all cases, a loose monolayer (80 $Å^2$) results in noticeable artifacts whereas a monolayer with standard specific surface leads to very reliable behavior well in accordance with experimental data. Despite their different insertion depth, the two peptides exhibit identical lytic efficiency. This is very likely a direct consequence of the very strong Van der Waals interactions between the fatty alkyl chains of the lipids and the highly lipophilic lower part of the peptide, resulting in an identical thinning of the two monolayers.

Keywords: Amphipathic peptides L_iK_j; Molecular dynamics; Monolayer; Peptide–lipid interaction

1. Introduction

It is of great importance to study peptide–lipid interactions in order to understand numerous biological reactions which take place at membrane surfaces such as the insertion and the folding of membrane proteins, the action of antibiotic peptides and the leakage of membranes by toxins. Cytolytic toxins are very common peptides and proteins which are widely distributed throughout the living world. Toxins can be classified as offensive or defensive, antibacterial, hemolytic, myotoxins or cardiotoxins but they can also be classified according to the type of damage they induce in cells. Among these toxins, one can find the toxins having in common an amphipathic α-helical structure. They are generally referred to as 'direct lytic factors' as opposed to toxins having an enzymatic activity. The amphipathicity can occur in several ways and here we will focus only on 'secondary amphipathic' peptides, i.e., peptides in which the potential amphipaticity is only revealed by a proper folding of the polypeptide backbone (α-heli-

* Corresponding author. Fax: +33-5-5796-2215;
E-mail: michel.laguerre@iecb-polytechnique.u-bordeaux.fr

0005-2736/01/$ – see front matter
PII: S0005-2736(01)00343-1

ces or β-sheets). Abundant literature has now established that an α-helix structure is a major requirement for cell lysis [1,2]. β-Sheet structures are also involved but with very different peptides [3,1]. In order to reproduce the behavior of natural amphipathic peptidic toxins like melittin [4], δ-hemolysin, bombolittin and defensin, artificial toxins designed with a minimalist approach were synthesized: only two amino-acids were used, the most lipophilic (L) and the most hydrophilic (K), also with a 2:1 L/K ratio, these peptides are designed to have a single charged K residue per putative α-helical turn to generate ideally amphipathic helices. Like natural peptides, the L_iK_j ($i=2j$) peptides are surface active because of their secondary amphipathic character and they have been shown to be more efficient than natural peptides [5]. In this last work it has also been proved that peptides longer than 12 residues fold into α-helices at interfaces, as expected, while shorter petides (from 9 to 5 residues) form intermolecular antiparallel β-sheets. Indifferently of their respective structure (α-helix or β-sheet) and of the quite different perturbations induced on lipids during their insertion, the lytic activity of these synthetic peptides was found to be very high [6,7]. Both structures exhibit a flat interfacial orientation as proved by PMIRRAS studies (Polarization Modulation IR Spectroscopy) [7]. Briefly, PMIRRAS combines Fourier transform infrared reflection spectroscopy with fast modulation of the incident beam between parallel and perpendicular polarization. Transition moments located in the interface plane give strong and upward oriented bands, while transition moments perpendicular to the interface give weaker and downward oriented bands [8,9]. From amide I and amide II spectral region (1500–1800 cm^{-1}), it is therefore possible to obtain structural and orientational in situ information on peptides embedded in monolayers formed at the air/water interface of a Langmuir trough.

However, a characterization in parallel at the molecular level is necessary to clearly understand the interaction of a peptide with a lipidic film and to gain insight on the important factors involved in the lytic mechanism. Computer simulations of detailed all-atoms models represent now a powerful approach and, in recent years, numerous molecular dynamics (MD) studies of peptides interacting with explicit membranes have been reported [10–15]. The aim of the present work is to address the question of the interaction between an amphipathic peptide in the L_iK_j series and a phospholipid monolayer (here DMPC). As the difficulty of the MD simulation is the large calculation time necessary to correctly reflect a short moment of the biological phenomena, we started with the peptides already located within the interface (and not outside the monolayer).

We have chosen two different peptides for this molecular dynamics study: a 'long' ideally amphipathic α-helical LK_{15} and a 'short' ideally amphipathic β-sheeted LK_9. The sequences, directly inspired from the work of Castano et al. [7], are the following:

LK_{15}: Dns-KLLKLLLKLLLKLLK and LK_9: Dns-KLKLKLKLK, with Dns = Dansyl.

In the particular case of LK_9, as the experimentally found structure is β-sheeted, the final L/K ratio was modified from 2:1 to 1:1 (ideally amphipathic β-sheet).

In the calculations the fluorescent probe has been conserved but due to the lack of correct parameters for the sulfamido group the dansyl moiety has been replaced by a benzoyl group. Four different models were built and were run for 1 ns each.

2. Theory and methods

2.1. Two simulation systems

One of the purposes of this study was to get insights on the influence of the lateral pressure exerted by the lipidic monolayer on the peptide secondary structure. It was then decided to build two different systems: one with a loose film and therefore a low lateral pressure (surface/lipid = 80 $Å^2$) and the other with a tight film and therefore a high lateral pressure (surface/lipid = 62.9 $Å^2$ close to natural surface for a fluid phase).

2.2. Computational details

2.2.1. Molecular mechanics

Calculations during the building of the systems were performed on a SGI Indy 4400 SC workstation running Macromodel version 5.0 (Columbia Univer-

sity, New York) [16] or on an Octane or an R10000 SGI workstation running InsightII and Discover ver. 97.0 (Molecular Simulations). Finally molecular dynamics simulations were carried out on a 4-processors SGI Origin 200 Server and took ~18 days/processor for a 1-ns simulation. Analysis was performed within DeCipher and Analysis modules of InsightII.

2.2.2. Peptide models

Models were first built within Macromodel. Conformational minima were found using the modified AMBER* (1992 parameters) force field as implemented and completed in the MacroModel program, the united atom force field was used with hydrogens really exprimed only on the heteroatoms and the aromatic rings (in order to insure correct atom parameters the dansyl group has been changed to a benzoyl group). Built structures were minimized to a final RMS gradient ≤ 0.01 kJ $Å^{-1}\,mol^{-1}$ via the Truncated Newton Conjugate Gradient method (TNCG, if $N_{atoms} \leq 750$) or the Polak-Ribière Conjugate Gradient method (PRCG, if $N_{atoms} > 750$) (1000 cycles). In all cases the extended cutoff option was selected (electrostatics = 25 Å, VdW = 25 Å, H-bond = 5 Å) and the GB/SA Solvation Model was used with water as solvent [17]. The corresponding minima were then exported towards InsightII after full hydrogen addition. In these conditions the following models were built: a LK_{15} molecule in an idealized α-helix conformation, and a β-sheeted antiparallel dimer of LK_9 (regular).

2.2.3. Peptide insertion in a Langmuir film model

A DMPC molecule was first built in MacroModel and minimized using the MM2* force field (1987 parameters), then all the torsional angles derived from the X-ray structure of DMPC, $2H_2O$ [18] were then applied to the previous structure. The resulting structure was then imported into InsightII, submitted to a semi-empirical quantum mechanics charge calculation (MOPAC/MNDO) and partitioned into neutral groups. A 13-Å spherical group-based cutoff was used throughout the calculations, as the neutral groups chosen are fairly large this cut-off is equivalent to a 13–20 Å atom-based cutoff. Calculations were then performed within Discover 97 with the Constant Valence force field (CVFF) as quoted above.

In all cases due to the software constraints, the membrane normal is oriented along the *y* axis. Periodic boundary conditions were applied in the *xyz* directions and a soft repulsive potential was applied on the top and the bottom of the box (ac surface) in order to simulate the interfaces (bottom of the trough and lipid/air interface) of an infinite planar layer. We used NPT conditions (i.e., constant number of particles, pressure, and temperature) in each simulation. The equations of motions were integrated with a time step of 1.5 fs, and the coordinates were saved every 1.5 ps (1000 steps), ac repulsive potential was on, constant pressure = 1 bar, equilibration = 1000 steps. The water model used was TIP3P [19,20]. Total run was 1 ns for each simulation. For all simulations, the average temperature was set to 300 K, i.e., above the gel–liquid phase transition of DMPC [21].

2.3. Construction of the microscopic model

Simulations were then carried out on two different systems: one for the LK_{15} peptide (A) and another one for the LK_9 (B) peptide. The two peptides were inserted in a DMPC monolayer fully solvated by water. In the simulation cell, the peptides were inserted into the monolayer just within the region of the phosphate–choline moieties.

2.3.1. Model I, specific lipid surface = 80 $Å^2$

A hexagonal crystalline monolayer of 50 lipids was first built (lipid surface = 40 $Å^2$) and roughly minimized, then half of the lipids were removed and the resulting monolayer (25 lipids, lipid surface = 80 $Å^2$) was inserted at the top of a $52 \times 65 \times 38.5$ $Å^3$ box (volume = 130 130 $Å^3$). Three DMPC molecules were removed in the center of the monolayer and the peptide molecule was docked in the gap, just at the interface. It has been shown that the molecular surface, S_{mol}, at the interface of a peptide can be approximated as follows: an antiparallel β-sheet parallel to the interface plane occupies roughly a surface of n (3.4 Å × 4.7 Å) = 16 n $Å^2$, where n is the number of residues, whereas a similarly oriented α-helix occupies a surface of n (1.5 Å × 12 Å) = 18 n $Å^2$. Thus, the LK_{15} molecular surface forming α-helix can be estimated to be around 270 $Å^2$ and that of the LK_9 forming β-sheet dimer to be around 288 $Å^2$. Then the

upper part of the box was filled with water (2493 H_2O) and the whole system was treated in periodic boundary conditions with minimum image option. The assembly was minimized using conjugate gradient method with the peptide backbone tethered until a RMS value ≤ 0.05. Then all constraints were eliminated and minimization was resumed until a RMS value ≤ 0.003 was reached. The whole system included from 10 391 atoms (α-helix, the net charge of the peptide is +4 *e*, model IA) to 10 475 atoms (β-sheet, the net charge of the peptide is +4 *e*, model IB).

2.3.2. Model II, specific lipid surface = 62.9 Å^2

The DMPC monolayer used in this model (cross-sectional area = 62.9 Å^2/lipid) was a fully prehydrated monolayer, previously minimized and submitted to a molecular dynamics run of 1 ns at constant pressure ($P = 1$ atm) at a temperature of 310 K (i.e., above the gel-crystalline transition state [14]). This layer (26 DMPC) was then inserted at the top of a $42.5 \times 65 \times 44.4$ Å^3 box (volume = 122 655 Å^3). As in Model I, three DMPC were removed just in the center of the monolayer and the peptide was docked in the gap, at the interface. We used the same minimization procedure to finally obtain two systems A (α-helix LK15) and B (β-sheeted LK9) including from 9652 atoms (α-helix, the net charge of the peptide is +4 *e*, model IIA with 2088 H_2O) to 9675 atoms (β-sheet, the net charge of the peptide is +4 *e*, model IIB with 2069 H2O).

3. Results and discussion

3.1. Cα RMSDs versus time for the two different systems

We have compared the Cα RMSD for the two systems A (80 Å^2) and B (62.9 Å^2) (Fig. 1). We can note that in the two systems the Cα RMSDs decrease during the first 200 ps which can be attributed to the equilibration of the system. After equilibration, the overall Cα RMSD value for the two systems seems to fluctuate in an almost identical manner except that we observe a slight and short increase for the LK_9 peptide around 500 ps. These two RMSDs graphs fluctuate from a minimum of

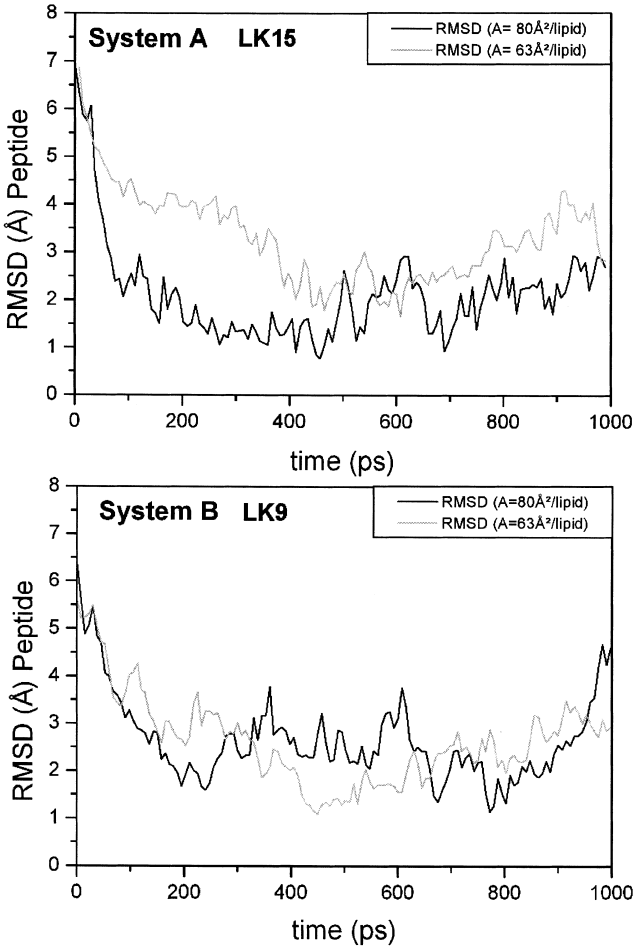

Fig. 1. RMSDs versus time for the Cα atoms in each simulation.

0.5 Å to a maximum of 2 Å with an average value around 1 Å: i.e., during their insertion in the monolayer the two different peptides kept their structure almost unchanged.

3.2. Fluctuations in structures

Fig. 2 plots a stroboscopic view of the peptides traces drawn every 50 ps for the four simulations.

For the system A, LK_{15}/DMPC, the major orientation change occurs very quickly in the first 100 ps with an initial extremely fast insertion step and afterwards the insertion proceeds very slowly with conservation of the same helical structure during all the remaining time of the simulation.

For the β-sheeted LK_9 peptide (system B), the first burst is no longer present and the insertion proceeds

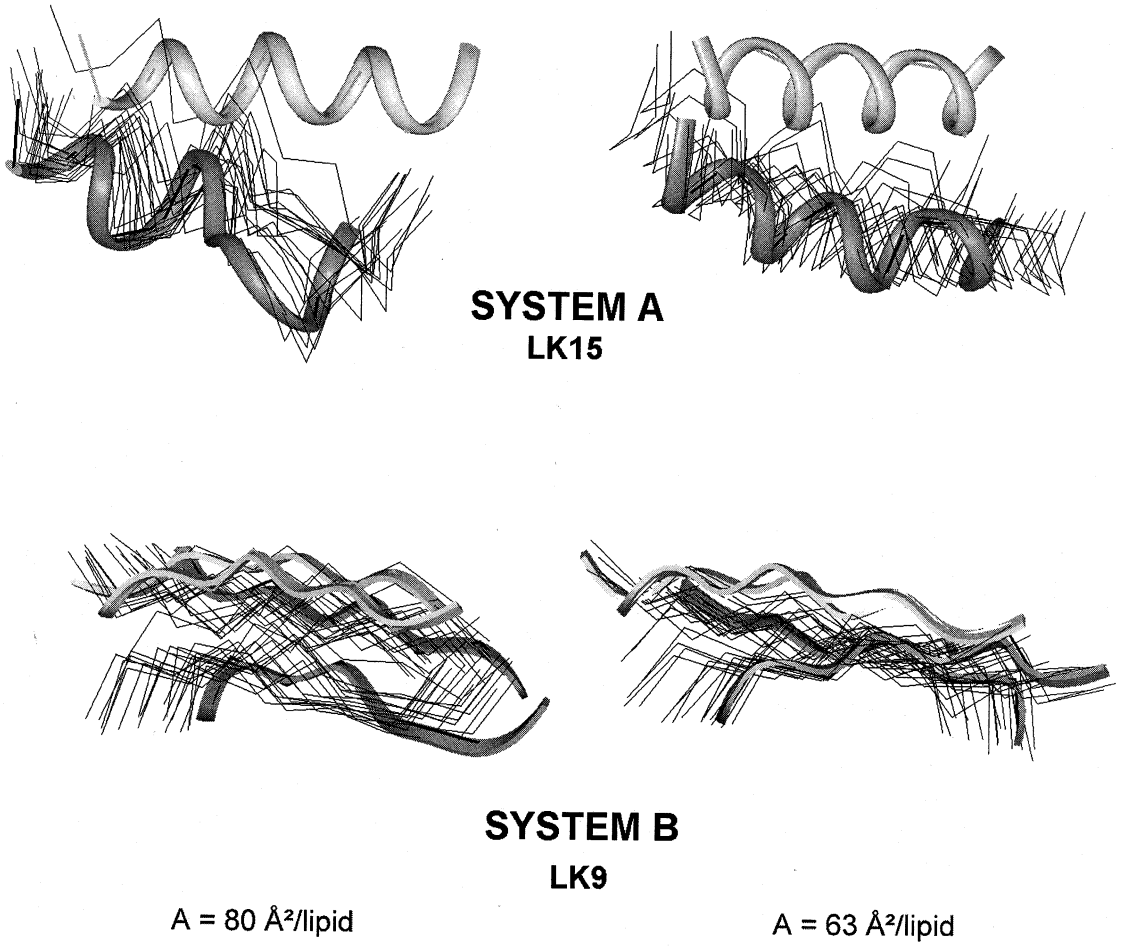

Fig. 2. Cα traces versus time, corresponding to structures saved every 50 ps, for (A) LK_{15}/DMPC and (B) LK_9/DMPC. Model I is at the left and model II is at the right. The vertical axis is the normal to the monolayer with water above and air below (reverse reality). Initial structure, light-gray ribbon; final structure ($t = 1000$ ps), dark-gray ribbon; intermediate structures, thin black lines.

very slowly without any discontinuous steps; the only difference is that with the large specific surface model I the peptide experienced a clear 'roll' according to its long axis whereas it inserts in a almost completely flat manner with the standard specific surface model II. This angle of roll was measured as a plane–plane angle between the horizontal plane (xOz) and the best-fit plane built on the β-sheeted dimer backbone (Fig. 3). With model I, the roll takes place immediately and quickly reaches, within 300 ps, a stable and high value of $43.1 \pm 2.5°$, and this is very likely a direct consequence of the low lateral pressure exerted by the lipidic monolayer in model I. On the other hand in model II (which is obvious in Fig. 2) the peptide dimer remains almost completely flat at the interface (angle of roll: $4.4 \pm 2.9°$).

3.3. Tilt angle during insertions

All experiments performed by PMIRRAS technique on the orientation of these peptides at the interface of lipid monolayers clearly led to the conclusion [7] that whatever the lateral pressure, their length and their secondary structure, the peptides are inserted within the monolayer in a flat manner (with an angle of tilt $\leq 30°$ which is the limit of sensitivity of the method). In Fig. 4, the evolution of the angle of tilt versus time is plotted for the four simulations. The tilt angle has been defined as a vector-plane angle between the horizontal plane (xOz) and a vector built as the best-fit of all backbone atoms either of the α-helix monomer or the β-sheeted dimer.

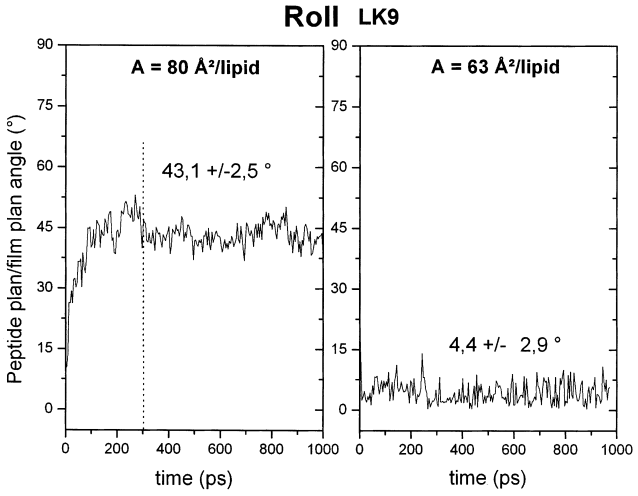

Fig. 3. Angle of roll of the LK_9 peptide during its insertion. Left, model IB; right, model IIB (angle between the horizontal plane and the backbone best-fit plane).

For the α-helix LK_{15} peptide the tilt value reaches its equilibrium very quickly (100 ps) and fluctuates smoothly during the remaining of the two simulations. With model I the equilibrated value is $21.8 \pm 3.5°$ but only $11.7 \pm 1.5°$ with model II. It is interesting to note that in the two simulations, the side which penetrates the monolayer is the Lys^{15}-CO-Ph end which tends to prove that the presence of the fluorescent probe linkage is far from being without consequence upon the behavior of the whole peptide.

In the case of the β-sheeted LK_9 peptide, the final value of the tilt is much lower, reaching only $10.2 \pm 3.0°$ with a low-pressure monolayer and hardly $1.5 \pm 1.1°$ with a high-pressure monolayer. As the LK_9 peptide is built with intermolecular antiparallel β-sheets the terminations of each sequence are balanced and the effect of the CO-Ph groups is less dramatic.

From these results which are in good accordance with PMIRRAS results, it can be concluded that, as for the orientational angles only, the two peptides, whatever their respective structures, are inserted in a similar way within a lipid monolayer with an almost flat orientation. The α-helix peptide experienced a slightly larger tilt but this is very likely a consequence of the high lipophilic nature of the fluorescent probe (this detrimental influence being largely reduced in the β-sheeted antiparallel dimer LK_9).

The results obtained from model II (standard specific surface) are as a whole in better agreement with experimental studies than the results from model I (high specific surface). It seems that a low lateral pressure exerted by the lipid monolayer (models I) will result in a slight unrealistic behavior of the peptides during their insertion: for instance the large 'roll' experienced by the β-sheeted LK_9 has never been found by PMIRRAS experiments [7] and the tilt value of the α-helix LK_{15} in this case is just at the limit of sensitivity of this technique.

3.4. Insertion of peptide in monolayer

After a careful examination of Fig. 2, it became obvious that the two peptides do not interact in the

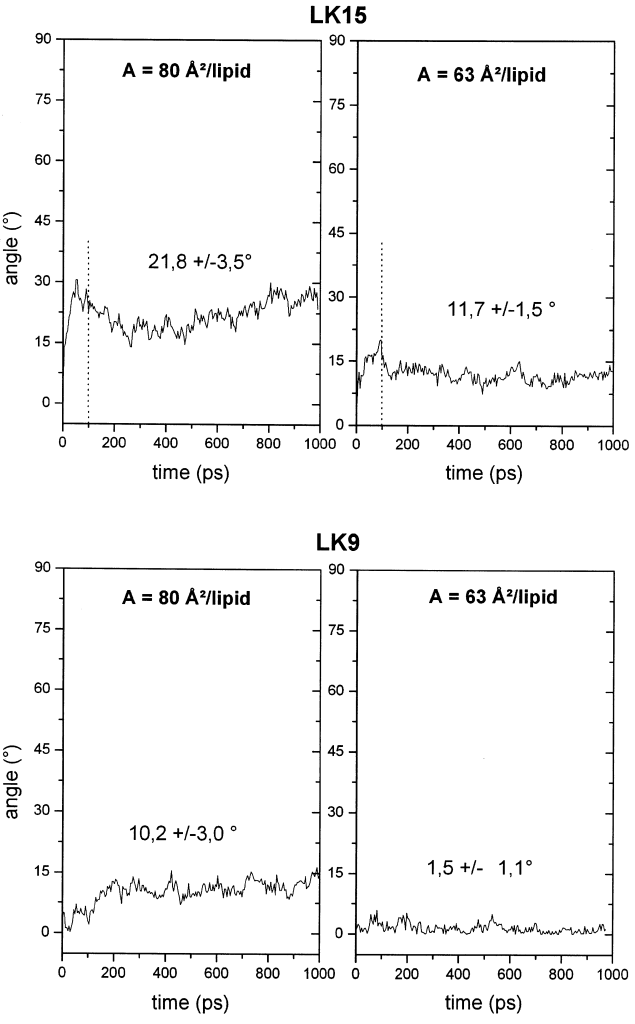

Fig. 4. Time variation of the angle of tilt of each lipid during their insertion. Up, LK_{15} peptide; down, LK_9 peptide; left, low-pressure model I; right, high-pressure model II.

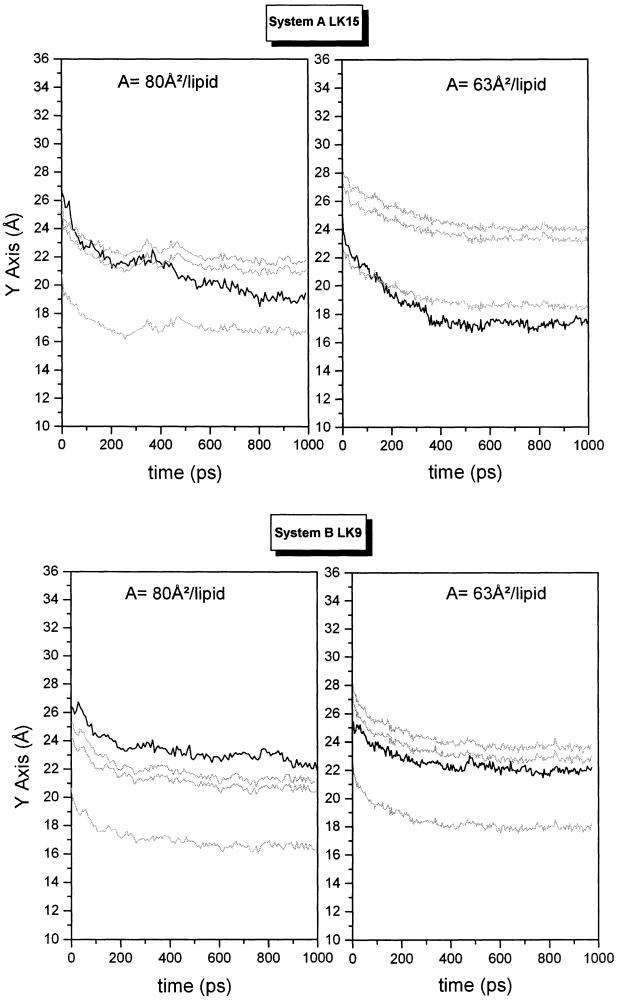

Fig. 5. Insertion of Cα of each peptide residues during the 1-ns simulation: up, system A LK_{15}; down, system B LK_9; left, low-pressure model; right, high-pressure model. The vertical axis is the normal to the monolayer with origin placed at the bottom of the periodic box, water being above and air at the bottom (reverse reality). Black line, trace of the average of the peptide C_α vs. time; gray lines, average of the main lipid atoms: up, nitrogen atoms, just below phosphor atoms; down, carboxy function.

same way with the lipid monolayer and that they do not insert within this monolayer at the same depth.

In fact in Fig. 5, we can follow the trajectory respectively for the ester carbonyl, phosphate and choline groups (average trajectory) for the DMPC lipids along with the average of the C_α atoms of each peptide. In the large specific surface model I, the peptide is initially positioned just above ($\sim$1 Å) the polar headgroups of the lipids (phosphates and ammoniums). However, in the standard specific surface model II this is no longer possible: due to the high pressure exerted by the lipid monolayer, the cavity where the peptide stands shuts down quickly enough to prevent the insertion of the peptide. Thus, in this model, the starting point of the peptide is slightly below ($\sim$2 Å) the polar headgroups of the lipids.

In the two models, the behavior of the peptide is strikingly different according to its secondary structure. The α-helical peptide inserts quickly and deeply in the lipidic monolayer as far as the carbonyl ester groups, on the other hand the β-sheeted peptide never inserts and remains just at the interface perturbing only the polar headgroups. This is in perfect accordance with the work of Castano et al. [7] where PMIRRAS technique clearly shown that β-sheeted peptides do not penetrate deeply in the monolayer, inducing only isotropic orientation of the PO_4^- lipid groups, whereas the α-helical peptides strongly perturb the C=O ester groups.

As already mentioned, the α-helical peptide experienced an immediate and very quick insertion step (5–6 Å insertion during 300 ps) followed by a very slow process (around 1 Å during the remaining of the simulation). Finally, and as mentioned in the work of Castano et al., everything happens as if the peptides push some lipid molecules. This is fairly obvious in Fig. 5 where, as a result of this pressure, the trace of the main atoms of the polar head groups of the lipids progressively goes down as the peptide inserts in the monolayer.

3.5. Secondary structure

A suitable and efficient way to explore the conservation or non-conservation of the secondary structure of these peptides during the molecular dynamics simulations is to plot Ramachandran graphs. The averaged Ramachandran plots have been drawn for the last 150 ps of each simulation (Fig. 6).

In all cases, the overall conformation either α-helix for LK_{15} or β-sheet for LK_9 is well conserved at the end of the simulations. We can note that the conformation of the β-sheeted LK_9 is slightly better retained than the α-helix LK_{15} with a larger number of spots in the region of the β-sheet compared to the

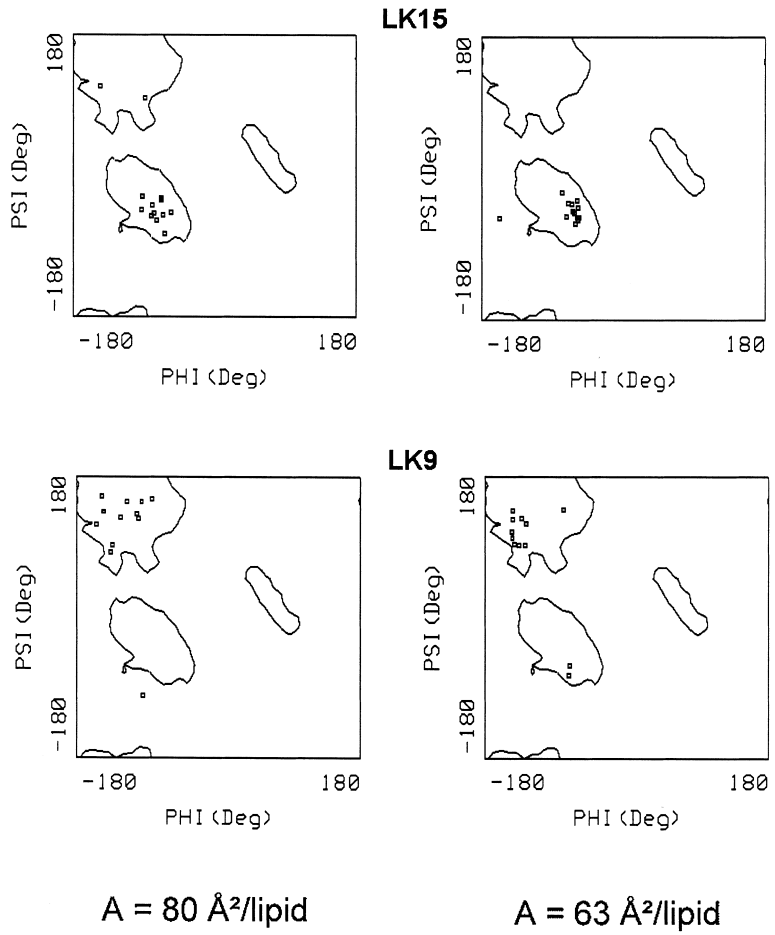

Fig. 6. Ramachandran plots of the two peptides LK_{15} and LK_9 during the last 150 ps of the simulations; left, low-pressure model I; right, high-pressure model II.

number of spots for the α-helix. For both structures, conformations are better conserved with models II with small specific surface and high lateral pressure, confirming again that a correct lateral pressure exerted by the lipidic layer is of crucial importance for an accurate study of a peptide dynamic behavior.

This fact is clearly illustrated by Fig. 7 where time-averaged values of backbone Ψ and Φ angles are drawn versus residue number for the four simulations. In the case of the large specific surface model I, the α-helix LK_{15} residues Leu^5 and Leu^6 show a disruption of the perfect helicity with backbone Φ and Ψ angles reaching values −120°, +140° for L5 and −90°, +100° for L6. This is no longer the case with the small specific surface model II, where the overall structure appears almost undisturbed. On an other hand, the β-sheeted LK_9 peptide seems less sensitive to the lateral pressure exerted by the lipidic layer: in both cases the same disturbance appears around K8 or L7 with a sign inversion for Φ only. This difference has no detrimental consequence as the overall structure of the peptide is not modified (see Fig. 2).

Overall, with a standard specific surface model, the two peptides retain their initial conformation when they insert within a lipid monolayer and this is in very good agreement with the experiment. Moreover in the case of the LK_{15} peptide, the hydrogen-bonding network clearly indicates that the final helix is, as experimentally found, always α and not π or 3_{10}.

3.6. Interaction of lipids with peptides

We have also been interested by the response of

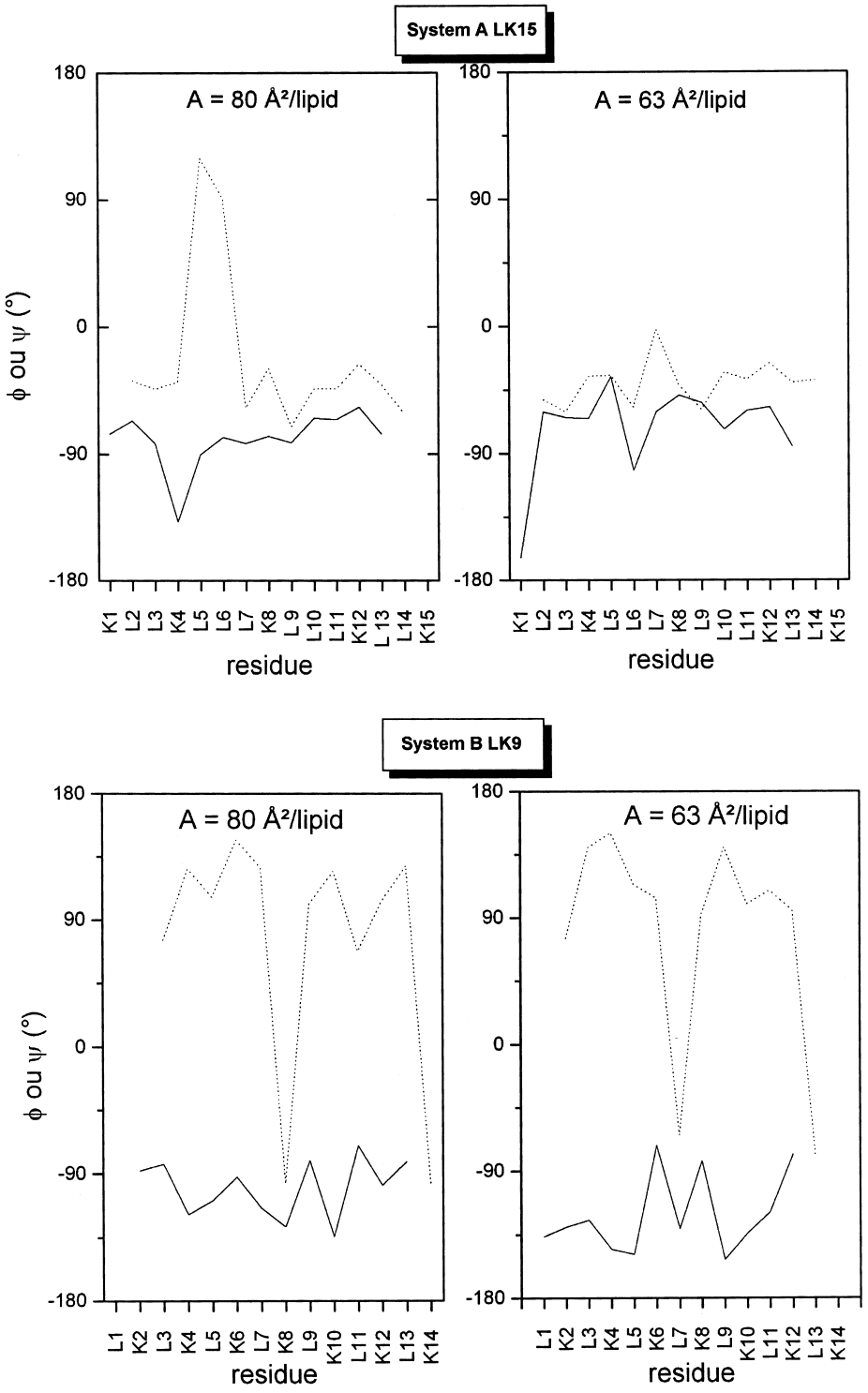

Fig. 7. Time-averaged values of backbone Ψ (solid lines) and Φ (broken lines) angles versus residue number. (A) LK_{15}/DMPC; (B) LK_9/DMPC. left, low-pressure model I; right, high-pressure model II.

the lipids to the peptide insertion. In order to depict accurately the final situation of the peptide within the lipid monolayer we have drawn in Fig. 8 the solvent-accessible surface according to the work of Connolly [22] at the beginning and at the end of the simulation for model II only. It is clear that, whatever their secondary structures are, at the end of the simulation the peptide is completely embedded in the lipidic monolayer. This is quite obvious from the views taken from the air/lipid interface: for both cases the peptides are completely concealed by the SN-1 and SN-2 chains of the DMPC due to very strong VdW interactions between the lipid aliphatic chains and the lipophilic side-chains of the two peptides. On the other hand, at the water/lipid interface, all hydrophilic side-chains of the two peptides kept a free access to water.

4. Conclusions

The interaction of synthetic amphipathic peptides of the L_iK_j series with fully hydrated DMPC monolayer was examined by molecular dynamics. It appears clearly that insertion took place in a very different way according to the secondary structure of the peptide. With an α-helix structure, the peptide inserts very deeply into the monolayer to the level of the fatty ester groups which are largely perturbed as evidenced by IR data [7]; on the other hand, with an antiparallel β-sheeted structure the peptide stays at the surface of the monolayer, disturbing only the ammoniums and phosphates groups. Whatever the secondary structure is, the peptides remain almost completely parallel with the horizontal plane. All these findings are in very good agreement with al-

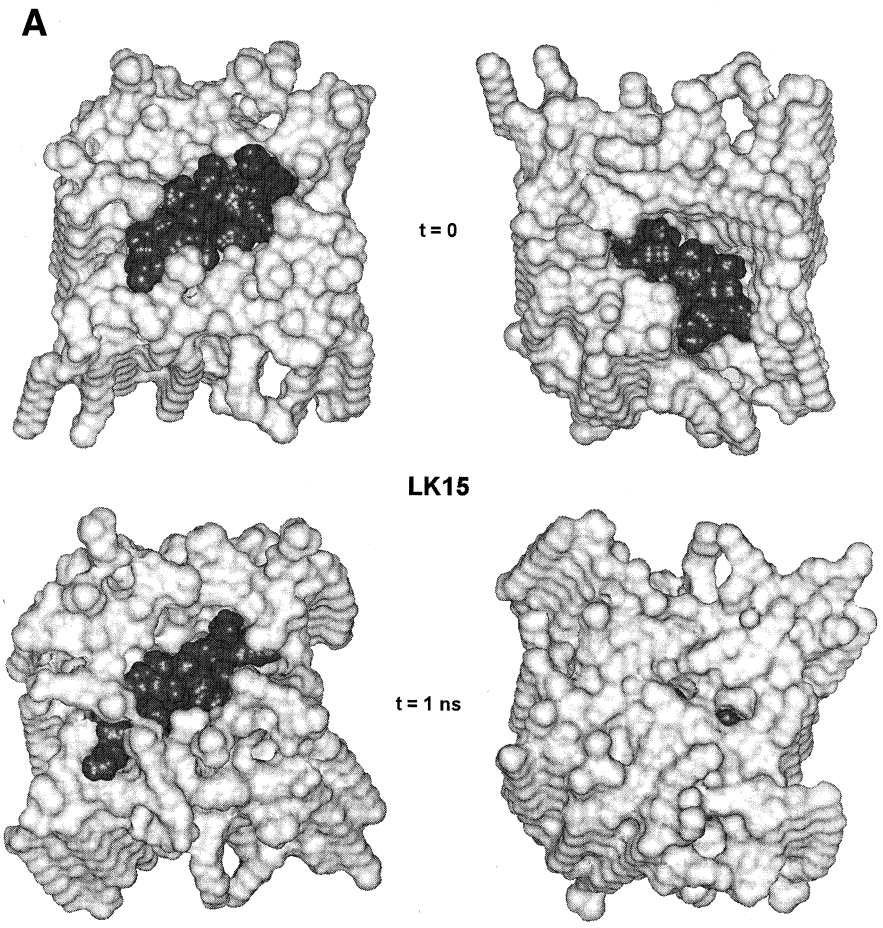

Fig. 8. Connolly surfaces (probe radius = 1.4 Å) of DMPC (light gray) and peptide (dark gray) for model II only before and after a 1-ns molecular dynamics run. (A) LK_{15}; (B) LK_9. first line, $t = 0$ ns; second line, $t = 1$ ns; left column, view of the interface from the water; right column, view from the alkyl chains.

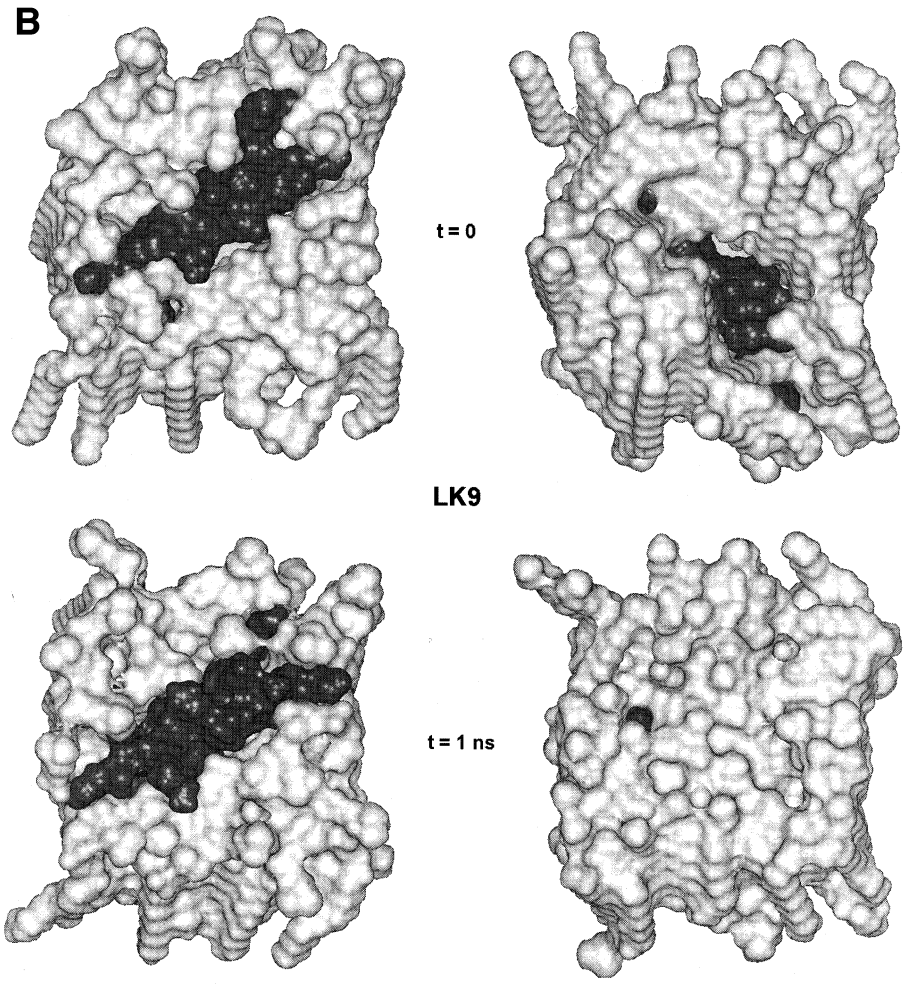

Fig. 8 (*continued*).

ready published experimental data [7]. Despite some difference in behaviors, a common phenomenon appears which may account for the identical lytic efficiency of these two series of peptides: because of a very strong Van der Waals interaction of the fatty acid alkyl chains with the highly lipophilic 'lower' part of the inserted peptide, the latter is almost complete buried inside the lipidic phase. This leads to a local but noticeable thinning of the monolayer, the same behavior having been shown recently by Bernèche et al. [14] during molecular dynamics simulation of melittin with a DMPC bilayer. These authors found that the hydrophobic core of the membrane is reduced by $\sim$30% from its original thickness near the center of the system. In our systems, locally where the insertion of peptide occurs, the global thinning can be estimated from 3.5 to 6 Å for a single monolayer. This may account largely for the lytic properties of these peptides, especially as it is reasonable to think that not only single peptide can insert but more likely rafts of peptides. Such a thinning on a large surface may have quite dramatic consequences on the membrane stability.

Also, it appears that a correct lateral pressure of the monolayer (i.e., a correct specific surface for lipids) is essential to perform reliable simulations. With low-pressure models, several large artifacts appear which may result in unrealistic behavior. It is clear that molecular dynamics simulation is highly sensitive to initial parameters and can lead to very different trajectories (and results) even in a simulation time as short as 1 ns.

References

[1] G. Saberwal, R. Nagaraj, Biochim. Biophys. Acta 1197 (1994) 109–131.
[2] T. Kiyota, S. Lee, G.V. Sugihara, Biochemistry 35 (1996) 13196–13204.
[3] R.M. Kini, H.J. Evans, Int. J. Peptide Protein Res. 34 (1989) 277–286.
[4] G. Colaccico, M.K. Basu, A.R. Buchelew, A.W.J. Berheimer, Biochim. Biophys. Acta 465 (1977) 378–390.
[5] S. Castano, I. Cornut, K. Büttner, J.L. Dasseux, J. Dufourcq, Biochim. Biophys. Acta 1416 (1999) 161–175.
[6] I. Cornut, E. Thiaudière, J. Dufourcq, in: P.D. Richard, M. Epand (Eds.), The Amphipathic Helix, CRC Press, Boca Raton, FL, 1993, pp. 173–219.
[7] S. Castano, B. Desbat, M. Laguerre, J. Dufourcq, Biochim. Biophys. Acta 1416 (1999) 176–194.
[8] D. Blaudez, J.M. Turlet, J. Dufourcq, D. Bard, T. Buffeteau, B. Desbat, J. Chem. Soc. Faraday Trans. 92 (1996) 525–530.
[9] D. Blaudez, T. Buffeteau, J.C. Cornut, B. Desbat, N. Escafre, M. Pezolet, J.M. Turlet, Thin Solid Films 242 (1994) 146–150.
[10] K.V. Damodaran, K.M. Merz Jr., B.P. Gaber, Biophys. J. 69 (1995) 1299–1308.
[11] P. Huang, G.H. Loew, J. Biomol. Struct. Dyn. 12 (1995) 937–956.
[12] T.B. Woolf, B. Roux, Proteins 24 (1996) 92–114.
[13] L. Shen, D. Bassolino, T. Stouch, Biophys. J. 73 (1997) 3–20.
[14] S. Bernèche, M. Nina, B. Roux, Biophys. J. 75 (1998) 1603–1618.
[15] K. Belohorcova, J.H. Davis, T.B. Woolf, B. Roux, Biophys. J. 73 (1997) 3039–3055.
[16] F. Mohamadi, N.G.J. Richards, W.C. Guida, R. Liskamp, M. Lipton, C. Caufield, G. Chang, T. Hendrikson, W.C. Still, J. Comp. Chem. 11 (1990) 441–467.
[17] W.C. Still, A. Tempczyk, R.C. Hawley, T. Hendrickson, J. Am. Chem. Soc. 112 (1990) 6127.
[18] H. Hauser, I. Pascher, R.H. Pearson, S. Sundell, Biochim. Biophys. Acta 650 (1981) 21–51.
[19] W.L. Jorgensen, C. Jenson, J. Comput. Chem. 19 (1998) 1179–1186.
[20] W.L. Jorgensen, J. Chandrasekhar, J.D. Madura, R.W. Impey, M.L. Klein, J. Chem. Phys. 79 (1983) 926–935.
[21] H. Ichimori, T. Hata, H. Matsuki, S. Kaneshina, Biochim. Biophys. Acta 1414 (1998) 165–174.
[22] M.L. Connolly, Science 221 (1983) 709–713.